Available online at www.sciencedirect.com

SciVerse ScienceDirect

Ceramics International 38 (2012) 4783–4789

CERAMICS INTERNATIONAL

www.elsevier.com/locate/ceramint

# The corrosion resistance of microsilica-containing $Al_2O_3$–MgO and $Al_2O_3$–spinel castables

E.Y. Sako *, M.A.L. Braulio, V.C. Pandolfelli

*FIRE Associate Laboratory, Materials Engineering Department, Federal University of São Carlos, São Carlos, SP 13656-905, Brazil*

Received 26 January 2012; received in revised form 21 February 2012; accepted 22 February 2012
Available online 3 March 2012

## Abstract

Microsilica addition in $Al_2O_3$–MgO and $Al_2O_3$–spinel castables helps to improve their flowability and partially accommodate their residual expansion after firing. Nevertheless, there is a lack of conclusive statements in the literature regarding the effects of microsilica on one of the main requisites for steel ladle refractories: corrosion resistance. In the present work, the performance of alumina–magnesia and alumina–spinel with or without microsilica when in contact with a steel ladle slag was evaluated based on three aspects: the material's physical properties, its chemical composition and the microstructural features before the slag attack. According to the attained results, microsilica induced liquid formation and pore growth during sintering, favoring the physical slag infiltration. Moreover, due to this liquid, $CA_6$ was formed in the matrix, mainly for the $Al_2O_3$–spinel composition, which also favored the castable dissolution into the molten slag.

*Keywords:* C. Corrosion resistance; Microsilica; Spinel castables

## 1. Introduction

Microsilica, or silica fume, is a raw material of utmost importance in the production of a variety of refractory castables. Comprised by sub-micrometric amorphous $SiO_2$ particles ($D_{50} \sim 0.1$ μm) with spherical shape, it imparts a positive effect on the castable flowability, acting as a solid lubricant and reducing friction among the particles [1]. Additionally, in alumina–silica compositions, microsilica is added as a very reactive source for the *in situ* mullite ($3Al_2O_3 \cdot 2SiO_2$) formation, decreasing its initial reaction temperature [2,3].

In alumina–magnesia castables, microsilica is helpful to prevent two main usual drawbacks. Firstly, by interacting with the magnesia particles surface, it partially hinders the intrinsic brucite – $Mg(OH)_2$ – generation and, consequently, reduces the cracks and explosion risks associated with this hydrate formation and decomposition during the castable drying step [4,5]. Secondly, the microsilica presence in this system also leads to a certain amount of liquid at high temperatures, which helps to accommodate and control the *in situ* spinel ($MgAl_2O_4$) expansive formation [6,7].

However, such liquid generation may also lead to negative effects, such as spoiling the material's hot mechanical properties. This aspect is more evident in refractory castables containing calcium aluminate cement (CAC) as a binder, in which low melting point phases in the $Al_2O_3$–CaO–MgO–$SiO_2$ quaternary system are formed [6,8]. Moreover, some previous studies on this subject [9,10] showed that, due to the liquid presence, acicular calcium hexaluminate ($CaO \cdot 6Al_2O_3$ – $CA_6$) grains are preferentially crystallized in the matrix, which results in higher overall expansion values after firing. Considering these aspects, refractory producers carefully consider the addition of microsilica in cement-bonded compositions.

Another drawback of microsilica and the consequent liquid generation in cement-bonded $Al_2O_3$–MgO and $Al_2O_3$–spinel castables is related to the corrosion resistance. According to some authors [11,12], the presence of silica fume induces a liquid phase-controlled sintering during the material's pre-firing, which results in a microstructural coarsening (pores and grains growth). Thus, the generation of large pores in the matrix favors slag and molten metal penetration and, consequently, decreases the material's working life. Samaddar et al. [13] also

---

* Corresponding author.
*E-mail addresses:* eric.ysako@gmail.com (E.Y. Sako), vicpando@ufscar.br (V.C. Pandolfelli).

0272-8842/$36.00 © 2012 Elsevier Ltd and Techna Group S.r.l. All rights reserved.
doi:10.1016/j.ceramint.2012.02.066

Table I
Composition, water content and apparent porosity after firing (1500 °C/5 h) of the $Al_2O_3$–MgO and $Al_2O_3$–spinel castables with or without microsilica.

| Raw materials | Content (wt.%) | | | |
|---|---|---|---|---|
| | AM 1MS | AM 0MS | AS 1M | AS 0MS |
| Tabular alumina ($D \leq 6$ mm) | 62 | 63 | 62 | 63 |
| Tabular alumina ($D \leq 0.2$ mm) | 18 | 18 | 10 | 10 |
| Reactive alumina | 7 | 7 | – | – |
| Dead-burnt magnesia ($D \leq 45$ μm) | 6 | 6 | – | – |
| Pre-formed spinel ($D \leq 0.5$ mm) | – | – | 21 | 21 |
| CAC | 6 | 6 | 6 | 6 |
| Microsilica | 1 | – | 1 | – |
| Water content (wt.%) | 3.9 | 4.0 | 4.1 | 4.2 |
| Apparent porosity (%) after firing at 1500 °C/5 h | 23.1 ± 0.9 | 17.4 ± 0.4 | 20.0 ± 0.3 | 15.2 ± 0.5 |

found out that silicate phases are more easily dissolved in steel ladle calcium–aluminium–silicate slags than in alumina, therefore, its presence should be avoided. On the other hand, Yan et al. [14] reported that, depending on the content added to the $Al_2O_3$–MgO or $Al_2O_3$–spinel refractory composition, microsilica may actually increase the materials corrosion and penetration resistance. According to these authors, when using the right proportion of this component, a decreased porosity is attained during the castable sintering step, reducing the possible physical paths for the slag penetration. In addition, the $SiO_2$ dissolution into the molten slag increases its viscosity, which suppresses further infiltration.

Although the corrosion resistance is one of the main requisites for steel ladle refractories, conclusive statements about the effects of microsilica in this property for $Al_2O_3$–MgO and $Al_2O_3$–spinel castables have not been reported. Considering that this raw material is relevant for the improvement of many other properties, this work addresses the main features related to the different corrosion behaviors of alumina–magnesia and alumina–spinel compositions with or without microsilica addition when in contact with an aggressive steel ladle slag.

## 2. Materials and techniques

In order to evaluate the microsilica role on the corrosion resistance of cement-bonded refractory castables containing *in situ* or pre-formed spinel, four compositions were selected, as shown in Table I. AM 0MS and AM 1MS compositions are alumina–magnesia (*in situ* spinel forming) castables, differing only regarding the microsilica (971 U, Elkem Materials, Norway) content (0 and 1 wt.%, respectively), whereas AS 0MS and AS 1MS are alumina–spinel (pre-formed spinel containing) ones, without and with silica fume.

For all of them, tabular alumina (T-60, $D \leq 6$ mm, Almatis, Germany) was used as coarse aggregates and calcium aluminate cement (Secar 71, Kerneos, USA) as the binder. The *in situ* spinel formation was induced in the AM compositions by adding 6 wt.% of dead-burnt MgO (95 wt.% of MgO, $CaO/SiO_2 = 0.37$, Magnesita Refratários S.A., Brazil), which reacted with the reactive alumina (CL 370, $D_{max} \sim 10$ μm, Almatis, Germany) and the fine tabular alumina ($D < 200$ μm) during firing, resulting in 21 wt.% of $MgAl_2O_4$ in the matrix. The same amount (21 wt.%) of synthesized spinel (AR78, 78 wt.% of $Al_2O_3$, Almatis, Germany) was added to the AS castables in three different granulometric ranges ($D < 500$ μm, $D < 45$ μm and $D < 20$ μm).

Due to an efficient particle packing design, using the Alfred model and a particle packing coefficient $q = 0.26$, and the use of 0.2 wt.% of a polycarboxylate dispersant (BASF, Germany), the water content required for suitable shaping (70–80% flow under vibration) was very close for all castables (Table I), regardless of the microsilica presence. Therefore, the results obtained for the free microsilica castables were not affected by any workability problems.

After mixing, cylindrical samples (50 mm × 50 mm) with an internal hole (20 mm × 25 mm) were shaped for the static corrosion experiments. They were cured for 24 h at 50 °C in a humidity saturated environment, dried for another 24 h at 110 °C and pre-fired at 1500 °C (1 °C/min) for 5 h in order to result in the *in situ* phase formation. Afterwards, the samples were filled in with 10 g of a high-$FeO_x$ steel ladle slag (Table II) and the corrosion tests were carried out at 1500 °C for 2 h in air.

The corroded samples were cut and the slag corrosion indexes were measured on their cross sections using the Image J 1.42q software (Wayne Rasband, National Institutes of Health, USA), according to the procedure described by Sako et al. [15]. Scanning electron microscopy (SEM) images (JSM-5900 LV, the Netherlands) of the corroded and unreacted areas were attained in order to compare the castable microstructure before and after the slag attack, and identify the main corrosion mechanisms related to the microsilica presence.

The castable pore size distribution in the matrix was calculated by the Image J 1.42q software in SEM micrographs attained after firing at 1500 °C for 5 h, and the apparent porosity was measured according to the Archimedes technique in kerosene.

Table II
Chemical composition of the industrial steel ladle slag used for the corrosion experiments.

| Composition | MgO | $Al_2O_3$ | $SiO_2$ | CaO | MnO | $Fe_2O_3$ |
|---|---|---|---|---|---|---|
| Content (wt.%) | 4.9 | 1.7 | 7.5 | 34.2 | 3.6 | 43.6 |

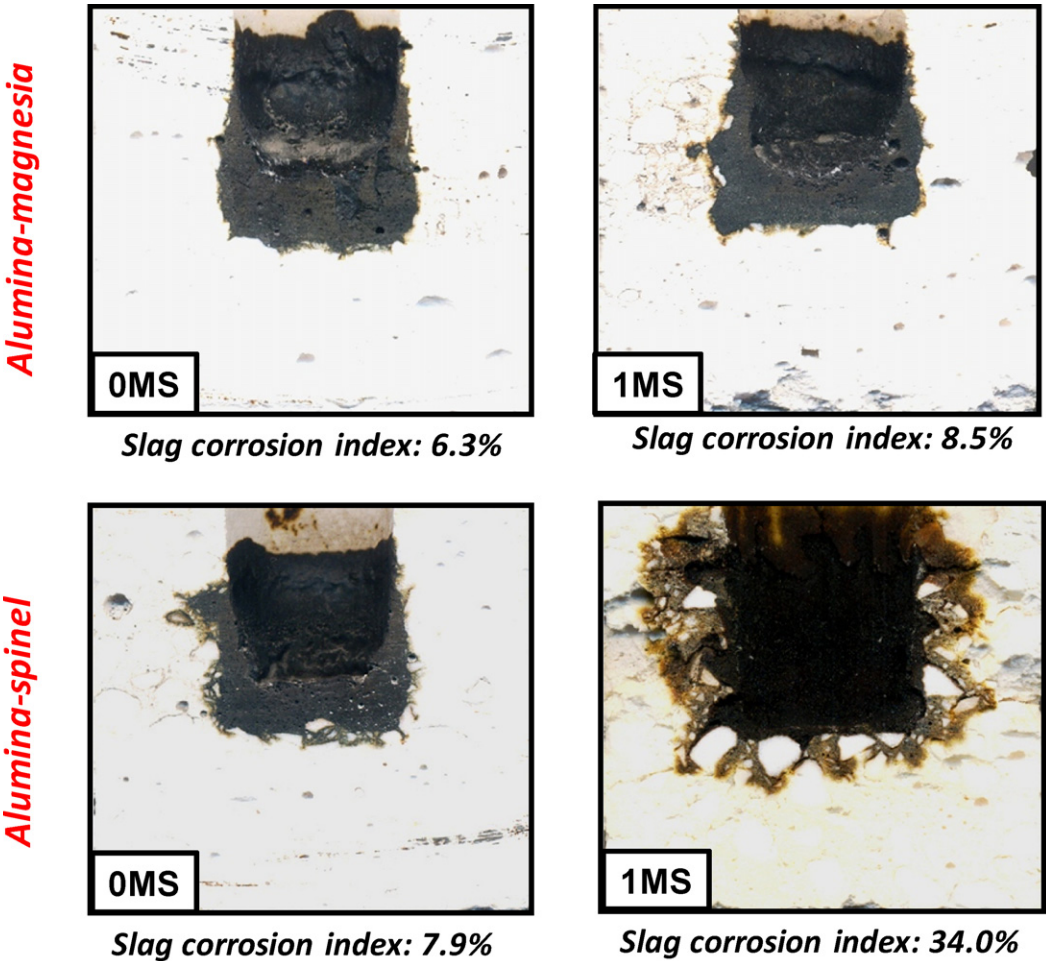

Fig. 1. Cross sections of the alumina–magnesia (AM) and alumina–spinel (AS) castables with 0 or 1 wt.% of microsilica after the corrosion experiments at 1500 °C for 5 h.

## 3. Results and discussions

The samples cross sections of the $Al_2O_3$–MgO and $Al_2O_3$–spinel castables with 0 or 1 wt.% of microsilica after the slag attack for 5 h at 1500 °C are shown in Fig. 1. As clearly observed, for both systems the silica fume addition reduced the materials' chemical performance, resulting in higher values of slag corrosion index, mainly for the AS composition.

According to Lee and Zhang [16], the corrosion of a refractory ceramic by any molten slag is defined by the material's physical properties, its chemical composition and the microstructural features before the slag attack. In a previous study [15], the performance of spinel castables was mainly ruled by the latter parameter. Therefore, in order to check how the castable's microstructure changed in the presence of microsilica, Fig. 2 shows SEM images of the evaluated castables attained after firing at 1500 °C for 5 h, before the slag attack. In the absence of microsilica, both alumina–magnesia and alumina–spinel castables presented basically the same microstructural features: a matrix comprised only by spinel and a high concentration of $CA_6$ crystals at the border of tabular alumina aggregates. When microsilica was present, calcium hexaluminate was generated at the aggregates and in the matrix, for the AM composition, and only in the matrix for the AS one.

The different microstructural evolutions of the AM 1MS and AS 1MS castables was already discussed by Sako et al. [17] and is related to the complex $CA_6$ formation mechanism. According to these authors, in silica-containing systems, $CA_6$ generates as a result of the decomposition of a ternary precursor phase, the $CM_2A_8$ ($CaO \cdot 2MgO \cdot 8Al_2O_3$), which derives from the previous reaction between spinel (either *in situ* or pre-formed) and a liquid in the $Al_2O_3$–CaO–$Na_2O$–$SiO_2$ quaternary system at roughly 1300 °C. Thus, as the spinel grains indirectly take part in the $CA_6$ formation mechanism, its previous distribution in the castable also rules the $CA_6$ location after firing at 1500 °C. For the AS 1MS composition, pre-formed spinel addition was carried out only in the matrix and, thus, the $CA_6$ is only found among the fine particles (Fig. 2). Conversely, for the IS castable, *in situ* spinel was formed all over the microstructure due to the faster $Mg^{2+}$ diffusion, which consequently led to the formation of $CA_6$ at the border of the alumina aggregates and in the matrix (Fig. 2).

In the silica-free compositions, however, the liquid which governs the above-mentioned mechanism was most likely not present at lower temperatures. Consequently, as the spinel

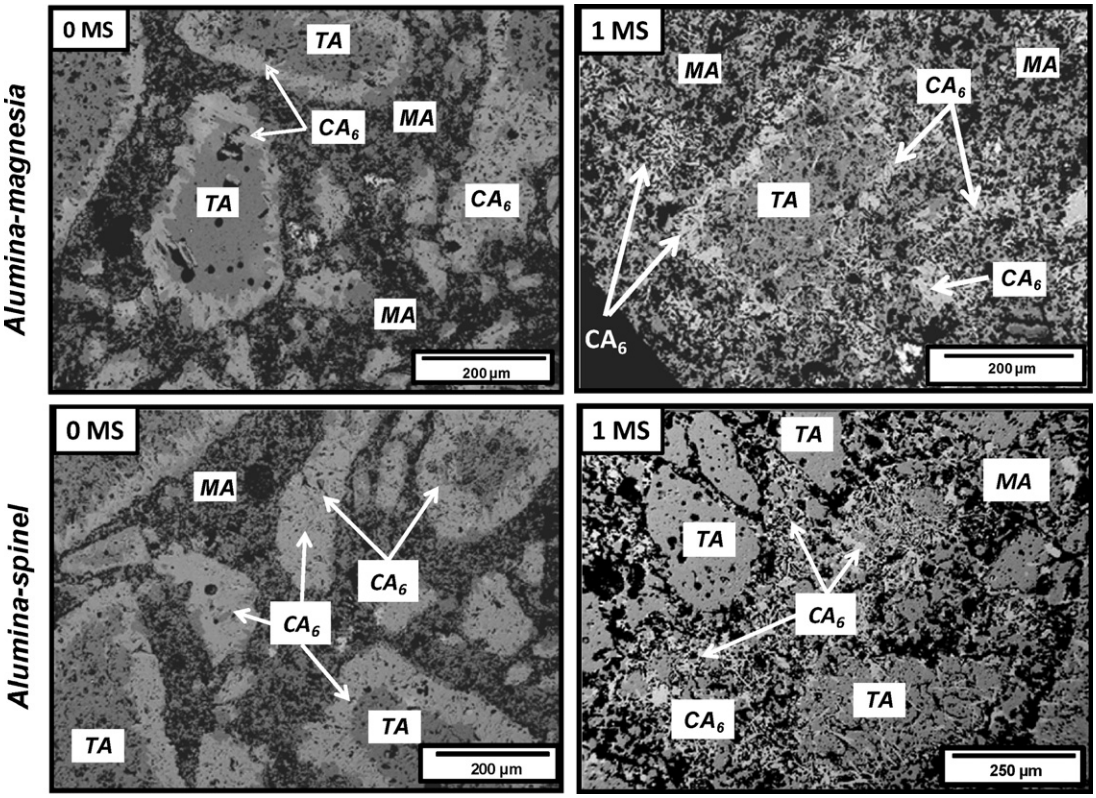

Fig. 2. Microstructure of the alumina–magnesia and alumina–spinel castables with 0 (0 MS) or 1 wt.% (1 MS) of microsilica after firing at 1500 °C for 5 h. TA, tabular alumina; MA, magnesium aluminate spinel.

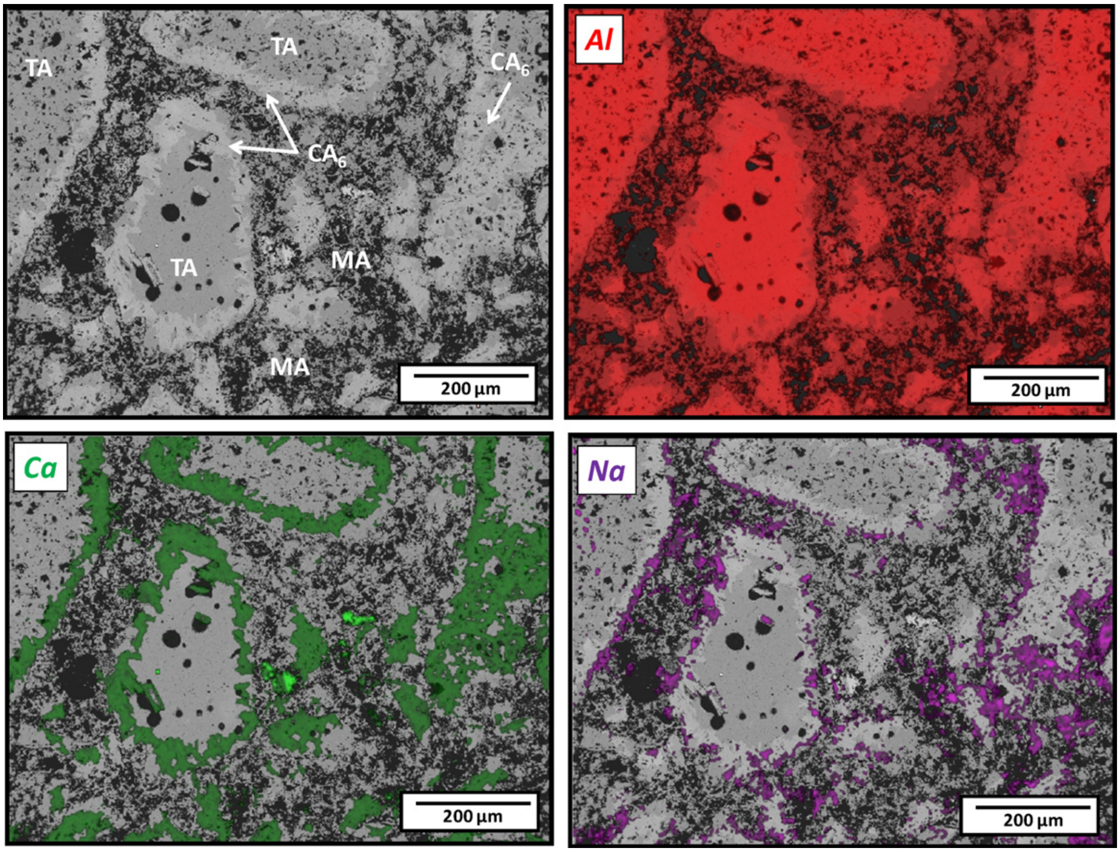

Fig. 3. EDS elements mapping of the alumina–magnesia castable without microsilica (AM 0MS) after firing at 1500 °C for 5 h.

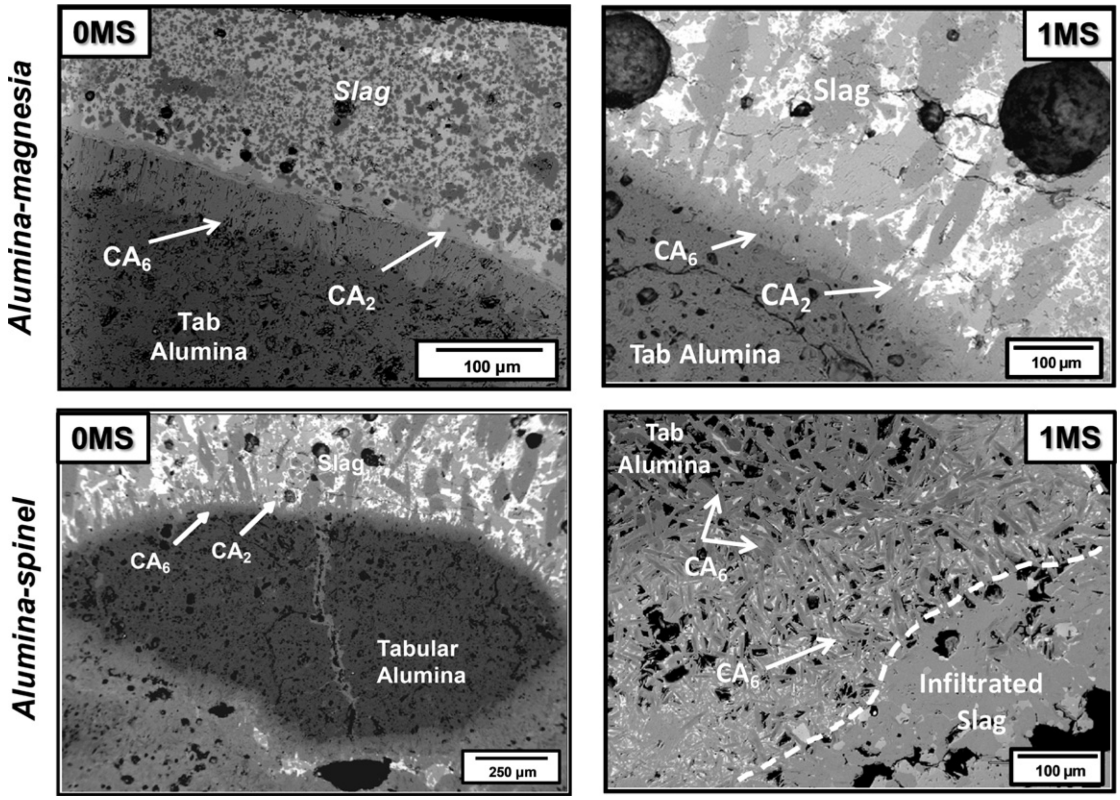

Fig. 4. Microstructure of the corroded samples, highlighting the different interactions between molten slag and tabular alumina aggregates according to the microsilica content. The dashed lines indicate the former borders of the aggregates before the slag attack.

phase did not take part in the reaction route, the calcium hexaluminate crystals were similarly formed in both samples (AM 0MS and AS 0MS) as a result of the reaction between $CA_2$ (originated from the dehydration of CAC phases) and the tabular alumina aggregates. The preferential reaction at the aggregates took place due to the higher concentration of Na-β-$Al_2O_3$, a typical industrial Bayer alumina impurity [18], in those coarse grains. Sodium beta alumina presents the same crystalline structure of $CA_6$ [19], and, thus, can easily turn into Na-$CA_6$ by simply incorporating $Ca^{2+}$ ions as solid solution. In order to evaluate this aspect, Fig. 3 shows the results of an EDS elements mapping for the AM 0MS composition. The high concentration of sodium in the $CA_6$ crystals formed at the tabular alumina aggregates can be observed, attesting that different $CA_6$ formation mechanisms may occur when adding silica fume.

Besides being pointed as one of the main microsilica effects on the expansive behavior of such spinel-containing castables [9], the different microstructure features observed in Fig. 2 also played a relevant role on the castables corrosion resistance (Fig. 4). When coated by $CA_6$ crystals, the tabular alumina aggregates reacted with the high-CaO slag and generated a dense $CA_2$ layer as an indirect dissolution product at the interface. This compacted layer acted as a protective barrier against further infiltration, providing excellent slag corrosion indexes for the silica-free castables (AM 0MS and AS 0MS). As already reported [15], the interaction between the unreacted aggregates and the molten slag in the microsilica-containing materials gave rise to $CA_6$ as it is a more thermodynamically favorable product. Because the $CA_6$ formation is followed by expansion, an opposite situation was found: cracking and novel cycles of liquid infiltration, explaining the worse performance of the AS 1MS castable. For the AM 1MS, a suitable number of aggregates coated by $CA_6$ was detected before the slag attack and that is the reason for presenting a closer performance to the microsilica-free castables and not as poor as the AS 1MS one.

Additionally, the microsilica presence also affected two other important parameters for the corrosion resistance evaluation: the chemical composition and the physical properties. Regarding to the former, the main impact of silica fume is the liquid generation at high temperatures. Fig. 5 shows high resolution micrographs of the evaluated castables matrices after firing at 1500 °C, highlighting the presence of an intergranular $SiO_2$-containing liquid in the AM 1MS and AS 1MS compositions. According to some reports in the literature [14,16], during the corrosion testing, this previous liquid is easily incorporated into the slag, increasing the amount of infiltrating liquid and reducing the material's performance.

Fig. 6 shows the pore size distribution in the matrix for the alumina–magnesia and alumina–spinel castables with or without microsilica after firing at 1500 °C. Whereas the castables presented very similar pore size distribution regardless of the sort of spinel incorporation, this property was indeed affected by the microsilica presence. The average pore size of the silica fume-free samples was smaller, mainly due to the following aspects: the reduced grain and pore growth, as a

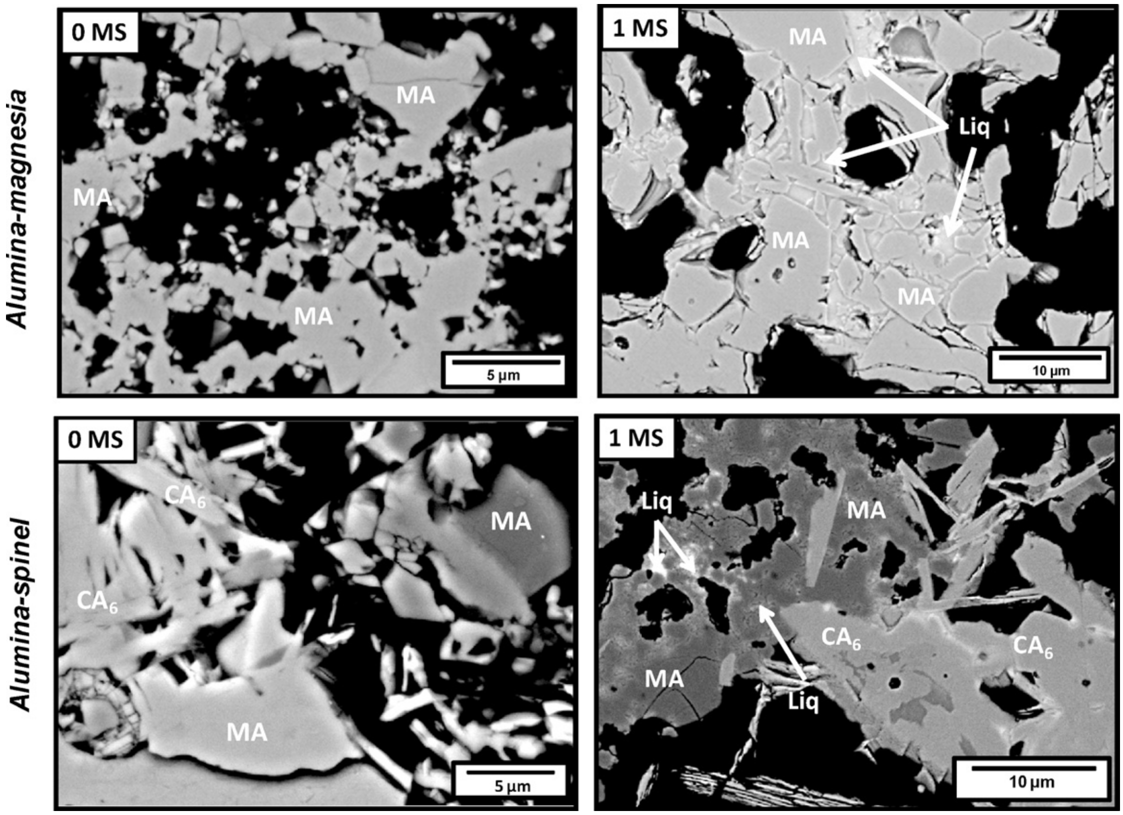

Fig. 5. Microstructure of the alumina–magnesia and alumina–spinel castables with 0 or 1 wt.% of microsilica after firing at 1500 °C for 5 h, pointing out the intergranular liquid presence in the microsilica-containing samples. MA, magnesium aluminate spinel; Liq, $SiO_2$-containing liquid.

consequence of a sintering process controlled by solid state mechanisms [11,12]; and the absence of acicular $CA_6$ crystals in the matrix, which usually leads to high expansion and an increased open porosity and average pore size [15]. Besides the results in Fig. 6, the above-mentioned $SiO_2$ effect on the castables physical properties can also be observed in Table I, which highlights the castables' apparent porosity after firing at 1500 °C/5 h.

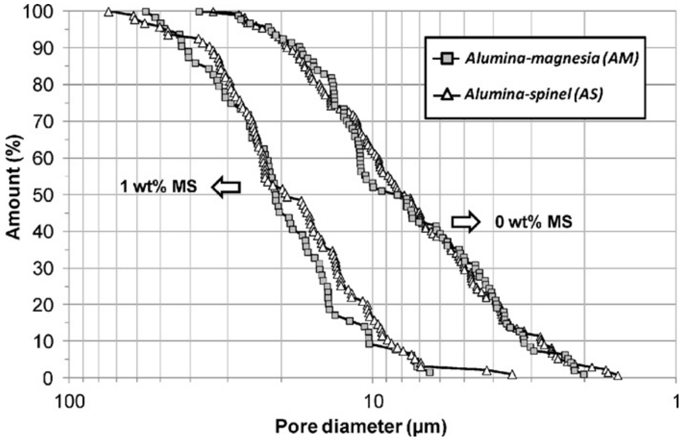

Fig. 6. Pore size distribution in the matrix of the alumina–magnesia and alumina–spinel castables with 0 or 1 wt.% of microsilica after firing at 1500 °C for 5 h.

The higher amount of smaller pores, the absence of liquid and mainly the favorable $CA_6$ formation at the tabular alumina aggregates hindered the molten slag penetration into the microsilica-free spinel castables, resulting in excellent slag corrosion indexes. The results pointed out that although presenting some important advantages, the use of microsilica for the production of spinel (*in situ* or pre-formed)-containing castables to be used in contact with steel ladle slag must be carefully analyzed, as it may spoil one of the main properties for this application, the corrosion resistance, as observed for the $Al_2O_3$–spinel composition.

## 4. Conclusions

The microsilica addition to cement-bonded $Al_2O_3$–MgO and $Al_2O_3$–spinel castables induces poor corrosion performance due to three different aspects:

- It reacts with the other raw-materials (mainly $Al_2O_3$, CaO and $Na_2O$) and generates a previous liquid in the castable microstructure, which, during the corrosion testing, is easily incorporated into the slag, increasing the amount of infiltrating liquid;
- Due to a liquid state-controlled sintering and the generation of acicular $CA_6$ crystals in the matrix, the microsilica-containing castables present higher pore size and apparent porosity,

respectively, after firing at 1500 °C/5 h. These microstructural features favor the liquid physical penetration;

- Finally, in the microsilica presence, $CA_6$ is usually formed in the castable matrix, mainly in the alumina–spinel composition. In this case, the tabular alumina aggregates are easily dissolved in the molten slag, increasing the slag corrosion index.

Therefore, the results showed that although mostly used to improve other properties, microsilica added to alumina–magnesia or alumina–spinel castables must be appropriately designed in order to ensure a suitable corrosion resistance. For steel ladle applications, silica fume-containing materials must be restricted for areas in which the slag attack is not an essential requirement.

## Acknowledgements

The authors are grateful to the Federation for International Refractory Research and Education (FIRE) and the Brazilian Research Funding CNPq for supporting this work.

## References

[1] B. Myhre, Microsilica in refractory castables—how does microsilica quality influence performance? in: Proceedings of Unified International Conference on Refractories, Orlando, USA, (2005), pp. 191–195.

[2] M.F.M. Zawraah, N.M. Khalil, Effect of mullite formation on properties of refractory castables, Ceramics International 27 (6) (2001) 689–694.

[3] B. Myhre, Hot strength and bond-phase reactions in low and ultralow cement castables, in: Proceedings of Unified International Conference on Refractories, São Paulo, Brazil, (1993), pp. 583–594.

[4] K. Ghanbari Ahari, J.H. Sharp, W.E. Lee, Hydration of refractory oxides in castable bond systems—I: alumina, magnesia, and alumina–magnesia mixtures, Journal of European Ceramic Society 22 (2002) 495–503.

[5] M. Rigaud, C. Xing, Basic castables for ladle's steel applications: a review, Journal of Canadian Ceramic Society 66 (3) (1997) 206–209.

[6] W.E. Lee, W. Vieira, S. Zhang, K.G. Ahari, H. Sarpoolaky, C. Parr, Castable refractory concretes, International Materials Reviews 46 (3) (2001) 145–167.

[7] M.A.L. Braulio, M. Rigaud, A. Buhr, C. Parr, V.C. Pandolfelli, Review: spinel-containing alumina-based refractory castables, Ceramics International 37 (6) (2011) 1705–1724.

[8] B.A. Vásquez, A. Caballero, P. Pena, Quaternary system $Al_2O_3$–CaO–MgO–$SiO_2$: II. Study of the crystallization volume of $MgAl_2O_4$, Journal of American Ceramic Society 88 (7) (2005) 1949–1967.

[9] E.Y. Sako, M.A.L. Braulio, D.H. Milanez, P.O. Brant, V.C. Pandolfelli, Microsilica role in the $CA_6$ formation in cement-bonded spinel refractory castables, Journal of Materials Processing Technology 209 (2009) 5552–5557.

[10] M.A.L. Braulio, L.R.M. Bittencourt, J. Poirier, V.C. Pandolfelli, Microsilica effects on cement bonded alumina–magnesia refractory castables, The Journal of the Technical Association of Refractories, Japan 28 (3) (2008) 180–184.

[11] A. Buhr, B.J. Baier, J.M. Aroni, R.W. McConnel, Raw material concepts for $SiO_2$ free strength castables in the temperature range up to 1200 °C, in: Proceedings of 45th International Colloquium on Refractories, Aachen, Germany, (2002), pp. 151–157.

[12] M.N. Rahaman, Grain growth and microstructure control, in: M.N. Rahaman (Ed.), Ceramic Processing and Sintering, Marcel Dekker Inc., New York, 2003, pp. 541–620.

[13] B.N. Samaddar, W.D. Kingery, A.R. Cooper, Dissolution in ceramic systems-11: Dissolution of alumina, mullite, anorthite, and silica in a calcium–aluminum–silicate slag, Journal of American Ceramics Society 47 (1964) 249–254.

[14] W. Yan, N. Li, B. Han, Influence of microsilica content on the slag resistance of castables containing porous corundum-spinel aggregates, International Journal of Applied Ceramics Technology 5 (6) (2008) 633–640.

[15] E.Y. Sako, M.A.L. Braulio, V.C. Pandolfelli, The corrosion and microstructure relationship for cement-bonded refractory castables, Ceramics International (2011), doi:10.1016/j.ceramint.2011.10.061.

[16] W.E. Lee, S. Zhang, Melt corrosion of oxide and oxide-carbon refractories, International Materials Reviews 44 (3) (1999) 77–104.

[17] E.Y. Sako, M.A.L. Braulio, E. Zinngrebe, S. van der Laan, V.C. Pandolfelli, In-depth microstructural evolution analyses of cement-bonded spinel refractory castables: novel insights regarding spinel and $CA_6$ formation, Journal of American Ceramic Society (2012), doi:10.1111/j.1551-2916.2012.05161.x

[18] P. Cichy, Fused alumina—pure and alloyed—as an abrasive and refractory material, in: L.D. Hart (Ed.), Alumina Chemicals Science and Technology Handbook, The American Ceramic Society Inc., Westernville, OH, 1990, pp. 393–426.

[19] L.R. Rothrock, Czochralski growth of single crystal sodium beta alumina, Journal of Crystal Growth 39 (1) (1977) 180–184.